

## Evaluation of Membrane Dynamics of IKAROS based on Flight Result and Simulation using Multi-Particle Model

By Yoji SHIRASAWA<sup>1)</sup>, Osamu MORI<sup>1)</sup>, Yasuyuki MIYAZAKI<sup>2)</sup>, Hiraku SAKAMOTO<sup>3)</sup>, Mitsue HASOME<sup>4)</sup>,  
 Nobukatsu OKUIZUMI<sup>1)</sup>, Hirotaka SAWADA<sup>1)</sup>, Saburo MATUNAGA<sup>3)</sup>, Hiroshi FURUYA<sup>3)</sup> and Jun'ichiro KAWAGUCHI<sup>1)</sup>

<sup>1)</sup>Japan Aerospace Exploration Agency, Sagamihara, Japan

<sup>2)</sup>Nihon University, Funabashi, Japan

<sup>3)</sup>Tokyo Institute of Technology, Tokyo, Japan

<sup>4)</sup>Tokai University, Hiratsuka, Japan

(Received June 28th, 2011)

Japan Exploration Agency (JAXA) launched a powered solar sail "Interplanetary Kite-craft Accelerated by Radiation Of the Sun (IKAROS)" on May 21, 2010. One of the primal technologies demonstrated at IKAROS is the spin-deployment of the sail whose diameter is 20 m class. After the launch, two-step deployment operation was performed and successful expansion of the sail was confirmed. This paper shows the flight data and observed dynamic motion during the deployment. At the quasi-static first stage deployment, the spin rate of main body shows little oscillation after each step and then damped quickly. The damping ratio of the spin rate after a later step of deployment is estimated by curve-fitting to be 0.0127. At the dynamic second stage deployment, the nutation motion is maintained within  $\pm 1.5$  deg/s and the spin rate of main body is converged quickly about 60s after the deployment start. These flight result and observed dynamic motion during the deployment are compared with the results of numerical simulations using multi-particle model. These results show that the multi-particle model can simulate the global behavior of membrane sufficiently except the dumping motion of in-plane oscillation between the main body and the expanded membrane.

**Key Words:** Membrane, Multi Particle Model, Solar Sail, Deployment, IKAROS

### Nomenclature

$d$	: cross section diameter of tether
$E$	: Young's modulus of membrane
$E_t$	: Young's modulus of tether
$F$	: inter-particle force
$F_d$	: damping force of vibration of membrane
$h$	: thickness of membrane
$I_{xx}, I_{yy}, I_{zz}$	: moments of inertia of main body
$I_{xy}, I_{yz}, I_{zx}$	: products of inertia of main body
$K$	: spring constant of membrane
$L$	: distance between two particles
$L_0$	: natural length of spring
$M$	: main body's mass
$\mathbf{r}_0$	: position vector of the root
$\mathbf{r}_1$	: position vector of the first node
$t$	: time
$(x, y, z)$	: coordinate frame fixed to main body
$(x_g, y_g, z_g)$	: center of mass of main body
$\alpha$	: coefficient of compression stiffness
$\beta$	: coefficient of dumping
$\theta$	: vibration angle of membrane
$\kappa$	: damping coefficient of vibration of membrane
$\nu$	: Poisson's ratio of membrane
$\rho$	: density of membrane

$(\omega_x, \omega_y, \omega_z)$  : angular velocity vector of  $(x, y, z)$  frame with respect to reference frame

### 1. Introduction

Japan Exploration Agency (JAXA) launched a powered solar sail "Interplanetary Kite-craft Accelerated by Radiation Of the Sun (IKAROS)" on May 21, 2010. This spacecraft is on a mission to demonstrate technologies required at extended solar power sail explore mission toward Jupiter and Trojan asteroids<sup>1)</sup>. One of the primal technologies demonstrated at IKAROS is the deployment of a large membrane in space. After the deployment operation was performed, successful expansion of the sail membrane was confirmed (Fig.1).

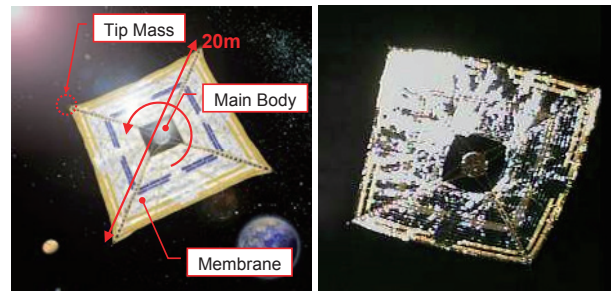


Fig. 1. IKAROS, left: illustration, right: image taken by a separation camera.

There are some methods to deploy a large membrane, and JAXA is studying the spinning type solar sail, in which the membrane is deployed and maintained flat by the centrifugal force. This method is expected to be realized with simpler and lighter-weight mechanism than other ways, because it does not require rigid structural elements. This method also has a risk of instability of main body's attitude or membrane's behavior.

It is very difficult to investigate the dynamics of membrane on the ground because it is greatly affected by air drag and gravity. To solve the problem, some experiments using high altitude balloon or sounding rocket have been conducted<sup>2,3)</sup>, however the free spin deployment of 20 m class of membrane was not experimented before the IKAROS flight.

The shape of the sail developed for IKAROS is a square which consists of four trapezoidal petals. The folding line of each petal is normal to the direction of centrifugal force. Four masses are attached to the four tips of the membrane by tethers to increase the centrifugal force and the inertial momentum of the sail. The sail is connected to the main body by tethers so as not to collide with the main body after the deployment.

Figure 2 shows the deployment method of membrane of IKAROS. The deployment sequence is divided into two major stages. Before the deployment, four petals of membrane are rolled around the main body and hold by four stopper guides. In the first stage, these stopper guides are rotated relatively around the main body by a motor. Then petals are extracted like a Yo-Yo despinner, and form a cross shape maintained by four stopper guides. In the second stage, these stopper guides are released, and four extended petals form a square shape. If the first stage deployment is performed dynamically, each petal will be twisted around the main body just after the deployment. Therefore the membrane needs to be deployed quasi-statically at the first stage. On the other hand, it is supposed to be deployed dynamically at the second stage.

Thus the deployment sequence in IKAROS consists of static first stage and dynamic second stage.

In order to analyze the dynamics of membrane and to organize a detailed deployment sequence, several numerical simulations using multi-particle model were performed before the launch. To find out the effect of the approximation on multi-particle model, numerical simulations using finite element method (FEM) model were also performed. This model was the finite element plane stress model based on the tension field theory, and employed implicit scheme based on the energy-momentum method<sup>4,5)</sup>. This model considered the effects of bending stiffness of components on the base membrane and the crease stiffness of folding line. The global behavior of the membrane calculated by multi-particle model was nearly equal to those calculated by FEM model<sup>6)</sup>.

However, these results have not verified sufficiently by experiment data of large flexible membrane in space environment. In this paper, the flight data of IKAROS is compared with the results of numerical simulation by multi-particle model, and the validity of the model is evaluated.

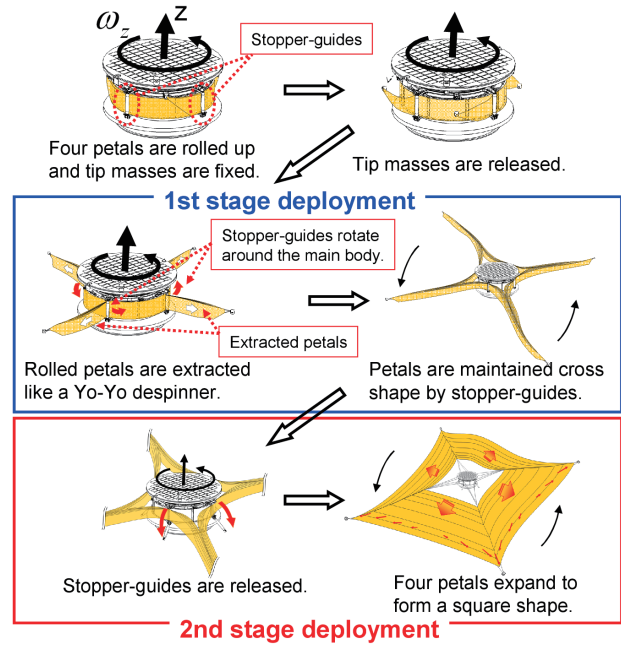


Fig. 2. Deployment sequence of IKAROS.

## 2. Multi-Particle Model

### 2.1. Mass-Spring model

In multi-particle model, each element of the membrane is assumed to be isotropic and substituted by particles connected by springs and dampers. This approximation facilitates the construction of model and lowers the computational cost. Mass of each particle is determined based on a designed value and actual measured value, and ununiform mass distribution of sail and difference of four petal's mass are considered.

The inter-particle force  $F$  can be described as following form:

$$F = \begin{cases} K(L - L_0) + \beta K\dot{L} & (L \geq L_0) \\ K\alpha(L - L_0) + \alpha\beta K\dot{L} & (L < L_0) \end{cases} \quad (1)$$

where  $K$ ,  $L$ ,  $L_0$ ,  $\alpha$  and  $\beta$  denote spring constant, natural length of spring, distance between two particles, coefficient of compression stiffness and coefficient of dumping, respectively. Assuming that the membrane resists a compression slightly, nonlinear spring model using coefficients of compression stiffness are employed. The spring constant  $K$  is determined by applying the principle of virtual work on an element so as to satisfy the relations of strain energy. This model assumes that the stress in the direction along each spring depends only on the strain in the same direction, so that the elasticity matrix is approximated to be diagonal. This model can also take into account the effect of bending stiffness of each element and crease stiffness of folding line by implementing rotational spring, however these characteristics have little effect on the global behavior of the membrane<sup>1)</sup>, and are not considered in this study. For the scheme of numerical time integration, the explicit Runge-Kutta-Gill method is employed.

### 2.2. Numerical model for IKAROS

Figure 3 illustrates the numerical model for IKAROS. Main body is modeled by rigid body, and membrane and tethers are modeled by mass-spring network. The coordinate frame  $(x, y, z)$  is fixed to the main body and its origin is set to the

geometric center of the main body. Parameters of the model are shown in Table 1. Since the coefficients of damping and compression stiffness are unknown parameters, these were changed comprehensively in pre-launch simulations to predict behaviors of membrane. The alignment of particles (mass points) and spring are different between first stage deployment model and second stage deployment model. The positions of particles and the connections of springs of a quarter part of the sail and tethers for each stage model are shown in Figs. 4 and 5, respectively.

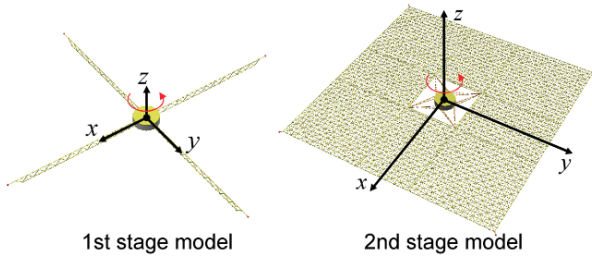


Fig. 3. Numerical model for IKAROS.

Table 1. Parameters of simulation model.

Parameter name	Symbol	Value
mass of main body	$M$	302.11kg
inertia moment of main body	$I_{xx}$	47.91 kgm <sup>2</sup>
	$I_{yy}$	47.46 kgm <sup>2</sup>
	$I_{zz}$	66.44 kgm <sup>2</sup>
product moment of main body	$I_{xy}$	-6.3x10 <sup>-4</sup> kgm <sup>2</sup>
	$I_{yz}$	4.6x10 <sup>-3</sup> kgm <sup>2</sup>
	$I_{zx}$	1.6x10 <sup>-3</sup> kgm <sup>2</sup>
center of mass	$x_g$	-1.6x10 <sup>-4</sup> m
	$y_g$	2.6x10 <sup>-4</sup> m
	$z_g$	-2.7x10 <sup>-2</sup> m
mass of membrane	$M_m$	14.253 kg
Young's modulus of membrane	$E$	3.0GPa
Poisson's ratio of membrane	$\nu$	0.4
density of membrane	$\rho$	1420.0 kg/m <sup>3</sup>
thickness of membrane	$h$	7.5 um
Young's modulus of tether	$E_t$	100.0GPa
cross section diameter of tether	$d$	0.73mm

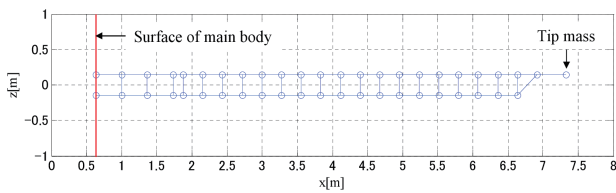


Fig. 4. Alignment of particles and springs of first stage model.

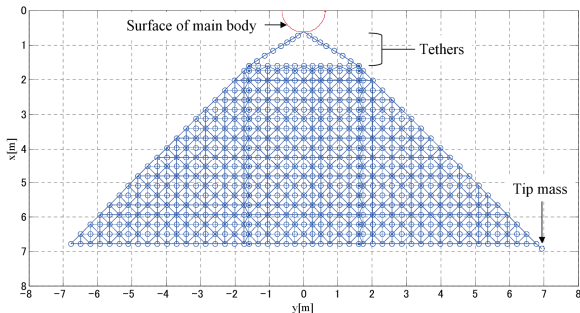


Fig. 5. Alignment of particles and springs of second stage model.

### 3. Result of Deployment Operation of IKAROS

This section describes the flight data and observed dynamic motion during deployment operation. After the launch of IKAROS on May 21, 2010, the membrane deployment operation was conducted as follows:

- May 26 Tip mass separation
- May 27~31 Spin up
- June 2 First stage deployment #1~2
- June 3 First stage deployment #3~6
- June 4 First stage deployment #7~9
- June 8 First stage deployment #10~11
- June 9 Second stage deployment

This operation was conducted checking the data of triaxial rate gyro and the images of monitor camera. Measurement resolution and sampling frequency of the rate gyro is 0.01 deg/s and 4 Hz, respectively.

#### 3.1. First stage deployment

Table 2 shows the operation result of the relative rotation angle of stopper guides within the first stage deployment. The operation was divided into 11 major steps.

Figure 6 shows the flight data of rate gyro within the first stage deployment. The horizontal axis represents the relative time from the generation of the first telemetry data of each operation day.

The value of  $\omega_x$  and  $\omega_y$  oscillate within  $\pm 0.4$  deg/s for each step with exception of step #11. The spin rate  $\omega_z$  decreases as the sequence proceed, and its oscillation is damped quickly.

On the way of step #11, the innermost part of membrane is deployed 2-dimensionally away from the surface of main body. This deployment becomes dynamically and raises an out of plane vibration with large amplitude. This motion is different from quasi-static deployment in previous steps.

The numerical model for first stage deployment used in this paper cannot simulate this motion. The model for second stage deployment may simulate this motion, however, it should consider the contact force among the particles, and this motion is not evaluated precisely in this study.

Table 2. Operation of the relative rotation of stopper guides.

Step No.	Rotation angle[deg]	Operating time[s]
#1	10.1	48
#2	21.3	52
#3-1	36.5	70
#3-2	51.7	70
#3-3	66.9	70
#4	112.5	190
#5	158.1	190
#6-1	203.7	190
#6-2	243.4	160
#7-1	294.9	212
#7-2	340.5	192
#8	386.1	202
#9-1	431.8	202
#9-2	471.0	166
#10	530.1	122
#11	570.0	86

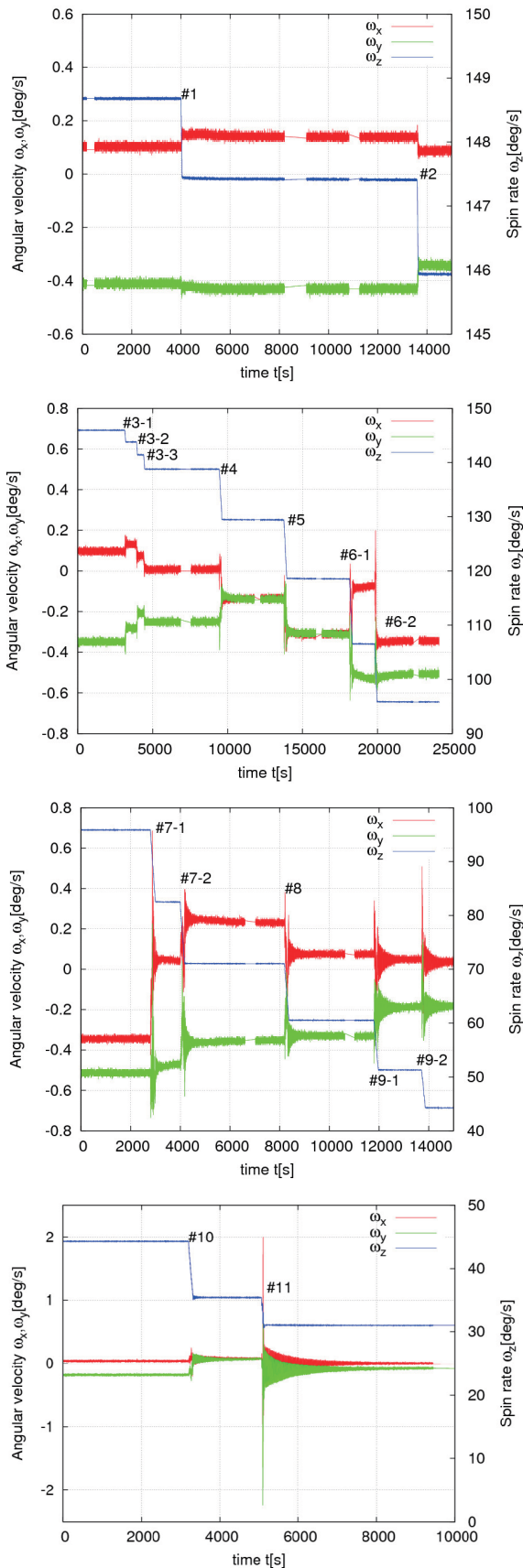


Fig. 6. Spin rate and angular velocity of main body during first stage deployment (Flight data).

### 3.2. Second stage deployment

Figure 7 shows the flight data of rate gyro within the second stage deployment. The deployment start time is  $t = 5908.449s$  in this figure. The value of  $\omega_x$  and  $\omega_y$  oscillate irregularly within  $\pm 1.5$  deg/s while 250s after the deployment start, and then converges to stable nutation with the amplitude of about  $\pm 0.5$  deg/s and the frequency of about 13.5 deg/s. This nutation motion is dumped gradually, and it takes more than 16000s to converge.

The center of oscillation of  $\omega_z$  seems to change from 18 deg/s to 15 deg/s at about 25s after the deployment start. From these data and images taken by monitor cameras, it is reasonable to consider that the second stage deployment was proceeded asymmetric and two of petals were not expanded until about 25s after the release of stopper guides. The cause of this deployment stuck is under the investigation. Though the membrane was deployed asymmetric and discontinuously, the sail was expanded completely.

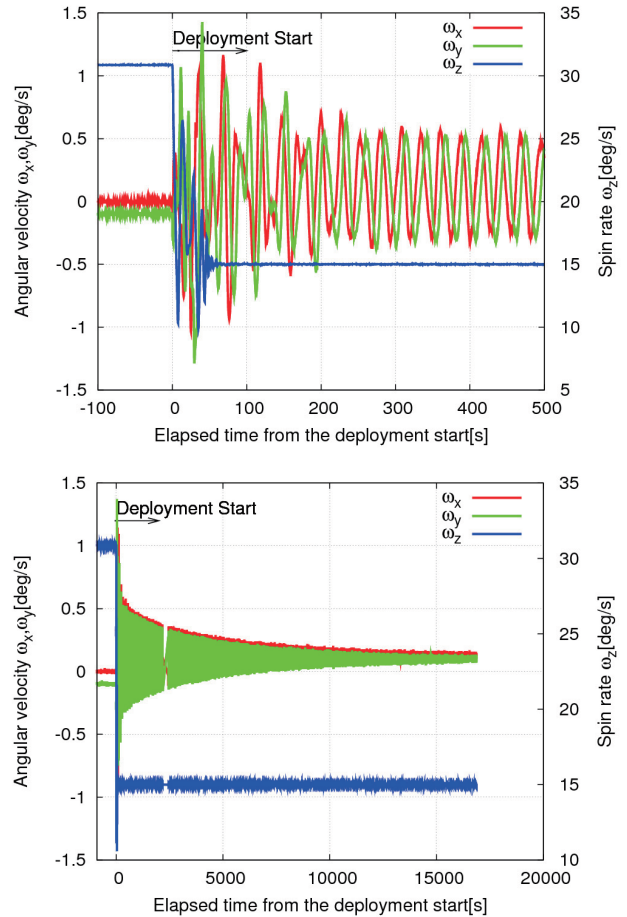


Fig. 7. Spin rate and angular velocity of main body during second stage deployment (Flight data).

## 4. Comparison of the Result of Multi-particle Model with the Flight Data

In this section, the results of simulation using multi-particle model are compared to the flight data.

### 4.1. First stage deployment

Figure 8 shows the variation of spin rate with respect to the



relative rotation angle. The decrease of spin rate of simulation result is smaller than the flight data. It would appear that there is an error of estimation of mass distribution for simulation model. To adjust the simulation result to the flight data, the authors derive a modified mass distribution model after several trial-and-error iterations, as shown in Fig. 9. In this figure, the horizontal axis represents each particle's position  $x$  and the vertical axis represents total mass of particles aligned at  $x$ . These values of  $x$  correspond to the alignment of particles of first stage model shown in Fig. 4. The red line represents the predicted mass distribution before the launch, and the green line represents the mass distribution modified based on the flight data. The error of spin rate after each step between the result of modified simulation model and the flight data is reduced to less than 0.5deg/s as shown in Fig. 8.

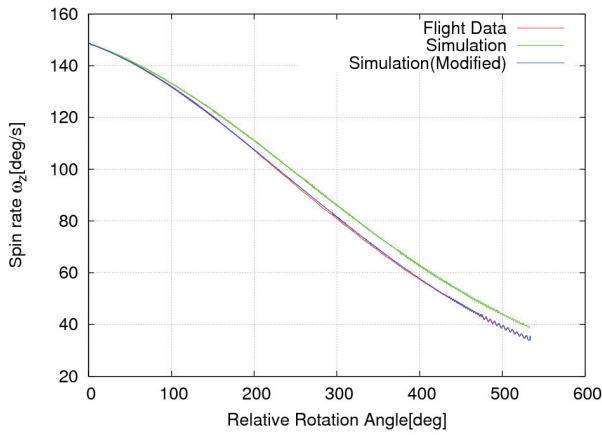


Fig. 8. Decrease of the spin rate with respect to the rotation angle during first stage deployment.

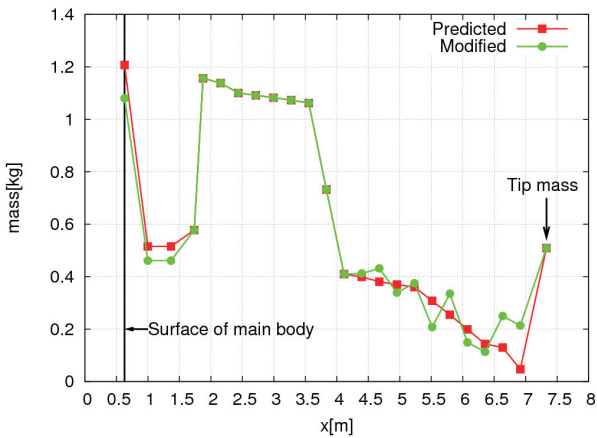


Fig. 9. Mass distribution of the particles in the first stage model.

Figure 10 shows the oscillation of spin rate after step #10. The spin rate of flight data shows little oscillation after each step and then damped quickly. The damping ratio of the spin rate after step #10 obtained by curve-fitting is about 0.0127. This quick damping can not be simulated by the multi-particle model though the coefficient of damping of membrane is varied over a wide range. To simulate this quick damping, the authors apply a damping force model which is proportional to the change rate of vibration angle of membrane. The concept of the model is illustrated in Fig. 11. The damping force  $F_d$  of

this model can be expressed as follows:

$$F_d = -\kappa \dot{\theta} \frac{(\mathbf{r}_1 - \mathbf{r}_0) \times \{(\mathbf{r}_1 - \mathbf{r}_0) \times \dot{\mathbf{r}}_1\}}{\|(\mathbf{r}_1 - \mathbf{r}_0) \times \{(\mathbf{r}_1 - \mathbf{r}_0) \times \dot{\mathbf{r}}_1\}\|} \quad (2)$$

where  $\kappa$ ,  $\mathbf{r}_0$  and  $\mathbf{r}_1$  denote the damping coefficient of vibration of membrane, the position vector of the root and the first node, respectively.  $\theta$  is the vibration angle of membrane defined as the angle between  $\mathbf{r}_0$  and  $(\mathbf{r}_1 - \mathbf{r}_0)$ . The result of simulation which employs this model with  $\kappa=0.4$  is also shown in Fig. 10. The damping ratio of the spin rate is obtained as 0.013, which is nearly equal to the one of flight data.

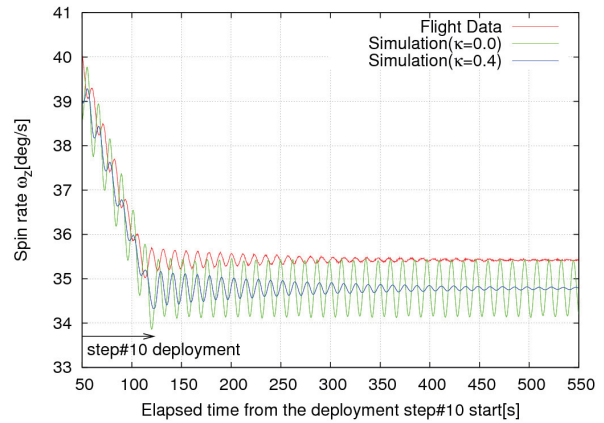


Fig. 10. Comparison of the damping of spin rate after step #10 of first stage deployment.

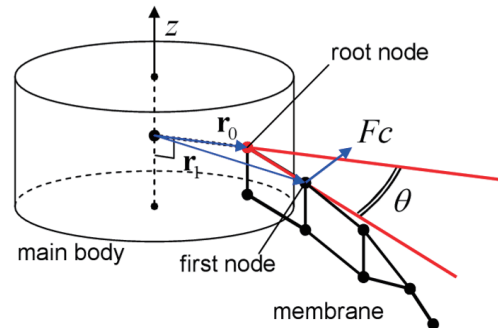


Fig. 11. Model of damping force proportional to the change rate of vibration angle of membrane.

Thus the modified multi-particle model can simulate the global behavior of main body during the first stage deployment well.

#### 4.2. Second stage deployment

As described in previous section, it is reasonable to consider that the second stage deployment was proceeded asymmetric and two of petals were not expanded until about 25s after the release of stopper guides. To simulate this feature of flight data of rate gyro, a simulation which appended a force of constraint that two petals not to expand for 26s after the deployment sequence start was performed. Figures 12 and 13 show the result of the simulation compared to the flight data. The amplitude of  $\omega_x$  and  $\omega_y$  of simulation is the same level of the flight data. The shift of center of oscillation of  $\omega_z$  of flight data is also well simulated by the model includes

the constraint.

The flight data shows the value of  $\omega_z$  is converged quickly about 60s after the deployment start. This quick dumping of the oscillation of  $\omega_z$  is not well simulated as shown in Fig. 13. A dumping coefficient  $\beta$  of membrane in this simulation is  $2.0 \times 10^{-4}$ s. Though it was much higher than that of normal case specified before the launch, the oscillation of  $\omega_z$  was not dumping so quickly as the flight data.

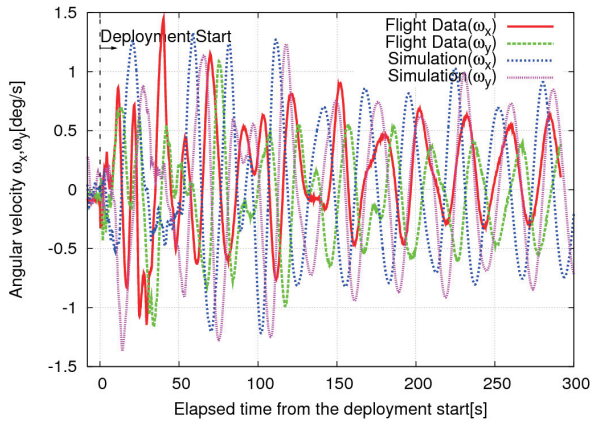


Fig. 12. Comparison of the angular velocity of simulation result and flight data at the second stage deployment.

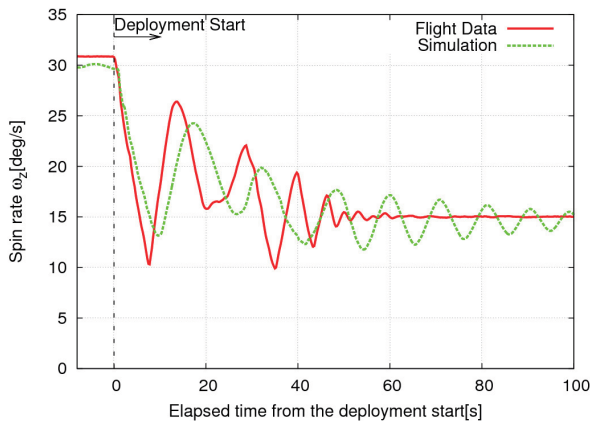


Fig. 13. Comparison of the spin rate of simulation result and flight data at the second stage deployment.

Figure 14 shows the variation of damping motion of  $\omega_z$  for different Young's modulus of membrane. These simulations are performed on the assumption that there is inaccurate estimation of the property of membrane. Figure 14 indicates that the oscillation of  $\omega_z$  damps quickly with increasing Young's modulus, however it still cannot simulate the quick damping of flight data. From these results, it is found that the difference of damping motion between the simulation results and flight data cannot be explained by an estimation error of a structural property of the membrane.

If the membrane's motion is affected by the strong dumping force, the membrane converges to the expanded shape quickly and then an in-plane oscillation between the main body and the membrane is induced. In such case, high tension is applied to the membrane and then the accuracy of prediction of

motion by multi-particle model would become worse because it uses diagonal approximated elasticity matrix. To simulate the dumping behavior with multi-particle model, some improvement would be needed.

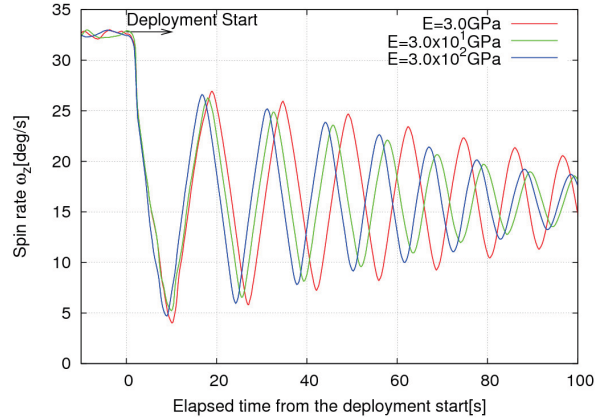


Fig. 14. Variation of damping motion of spin rate oscillation at second stage deployment for different Young's modulus of membrane.

## 5. Conclusion

JAXA launched a powered solar sail "IKAROS" on May 21, 2010 and succeed the deployment of membrane. In this paper, flight results of the deployment was reported and compared with the results of numerical simulations using multi-particle model. It was found that multi-particle model could simulate the global behavior of membrane well. However, the dumping motion of in-plane oscillation between the main body and the expanded membrane could not be simulated well. It was considered that the estimation error of a structural property of the membrane is not a main factor, and to simulate this motion well, some improvement would be needed. Outside of this exception, it can be said that the numerical analysis using multi-particle model is feasible to investigate the macro-dynamics of membrane.

## References

- 1) Mori, O., Sawada, H., Hanaoka, F., Kawaguchi, J., Shirasawa, Y., Sugita, M., Miyazaki, Y., Sakamoto, Y. and Funase, R.: Development of Deployment System for Small Size Solar Sail Mission, *Trans. JSASS Space Tech. Japan*, **7**, ists26 (2009), pp.Pd\_87-Pd\_94.
- 2) Tsuda, Y., Mori, O., Takeuchi, S. and Kawaguchi, J.: Flight Result and Analysis of Solar Sail Deployment Experiment using S-310 Sounding Rocket, *Space Technol.*, **26**(2006), pp. 33-39.
- 3) Nishimaki, S., Mori, O., Shida, M. and Kawaguchi, J.: Stability and Control Response of Spinning Solar Sail-craft containing A Huge Membrane, *57<sup>th</sup> International Astronautical Congress*, IAC-06-C1.1.07, 2006.
- 4) Simo, J. C. and Tarnow, N.: The Discrete Energy-momentum Method. Conserving Algorithms for Nonlinear Elastodynamics, *Journal of Applied Mathematics and Physics (ZAMP)*, **43** (1992), pp.757-792.
- 5) Miyazaki, Y. and Kodama, T.: Formulation and Interpretation of the Equation of Motion on the Basis of the Energy-Momentum Method, *Journal of Multi-body Dynamics*, **218** (2004), pp.1-7.
- 6) Miyazaki, Y. and Iwai, Y.: Dynamics Modeling of Solar Sail Membrane, *13<sup>th</sup> Workshop on JAXA Astrodynamics and Flight Mechanics*, A-6, 2004.